Structure of colloidal particles in water-oil mixtures stabilized by polymeric emulsifiers: 2. Small angle neutron scattering investigation

Françoise Candau, Jean-Michel Guenet, Jacques Boutillier and Claude Picot
CNRS Centre de Recherches sur les Macromolécules, 6, rue Boussingault, 67083 Strasbourg-Cédex, France
(Received 16 February 1979)

Small-angle neutron coherent scattering techniques have been used to characterize the conformation of amphiphilic macromolecules in polymeric microemulsions. The radius of gyration, the molecular weight and the aggregation number of the macromolecules within the micelles have been measured using a dilution procedure in conjunction with an adjustment of the contrast factor between polymer and solvents. Additional information on the internal structure of the micelles has been obtained from the asymptotic behaviour of the scattering form factor $P(q)$. From considerations of the respective affinities between the two copolymer sequences and the solvent mixture, plausible models are proposed for the micellar structure.

INTRODUCTION

The electron microscopy experiments reported in the preceding article[1] have shown that the transparent fluid mixtures water/toluene/2-propanol stabilized by polystyrene-poly(ethylene oxide) graft copolymers exist as a disperse assembly of spherical droplets ranging in diameter from 100 up to 500 Å. This size range is of the same order of magnitude as for conventional microemulsions formed from soap surfactants.[2-4] However, from dialysis experiments,[1] it was shown that, contrary to classical microemulsions, there is no evidence of trapping of one of the solvent mixture constituents in the micelles but rather a selective and partial absorption of the different components by the two sequences of the copolymer. As a result, both the continuous phase and the interior of the droplets consist of a mixture of the three solvents.

In this paper, we are interested in the investigation of the structural properties of the dispersed particles. Because of the small size range of these particles, small-angle neutron scattering (SANS) experiments are suitable for such an investigation.[5,6] However, there is a major difficulty arising from the complexity of the contrast factor which depends on the composition of both the copolymer[7,8] and the ternary solvent mixture.

Neutron scattering allows the scattering power of the two components of an object to be adjusted selectively by using protonated and deuterated molecules. The results obtained by this labelling method have led to major advances being made in the study of concentration effects in polymer solutions[9] and in the characterization of copolymers in dilute solutions.[7,8]

We have used this 'contrast adjustment method' between copolymer and solvents to determine the radius of gyration R_G and the molecular weight $M_{w,a}$ of the associated copolymer molecules in the micelles, in the 'Guinier' range ($q \cdot R_G \leqslant 1$ where the scattering vector $|q| = (4\pi/\lambda)\sin(\theta/2)$, λ is the wavelength and θ is the scattering angle). The last parameter $M_{w,a}$ leads to the micellar aggregation number of the copolymer. Supplementary information on the structural behaviour of copolymers in the micellar particles was also obtained from the form factor $P(q)$ which was investigated in the 'intermediate' range ($R_G^{-1} \leqslant q \leqslant l^{-1}$ where l is the length of a link of the macromolecule).

MATERIALS

In order to emphasize the influence of the amphiphilic nature of the copolymer, we performed our experiments on transparent systems prepared from two PS-PEO graft copolymer samples of different composition. Samples A7 and A4 have an identical PS backbone, but sample A7 possesses longer PEO branches, which gives it a more pronounced hydrophilic character (see *Table 1* of paper 1).

To illustrate the effect of the overall composition of the studied systems, we will consider, as for *EM* experiments, two compositions A and B located in the vicinity of the transition line, where A and B are toluene-rich and water-rich areas, respectively, and the two corresponding A′ and B′ systems are located far above the transition line (see *Figure 4* of paper 1).

EXPERIMENTAL

Small-angle neutron scattering experiments (SANS) were performed at the Institute Laue Langevin (ILL) in Grenoble on apparatus widely described in the literature.[6,10]

Measurements of the radii of gyration of copolymers were carried out in the Guinier range ($q \cdot R_G \leqslant 1$) on the D_{11} apparatus, for which the modulus of the scattering vector ranges from 5×10^{-3} to 1.8×10^{-2} Å^{-1}.

Studies in the intermediate domain ($q \cdot R_G \geqslant 1$) were performed on the D17 camera ($10^{-2} < |q| < 10^{-1}$ Å^{-1})

0032-3861/79/101227-10$02.00

Table 1 Dimensions and aggregation numbers of graft copolymers in the micellar particles determined from SANS experiments

	Toluene-rich side					Water-rich side				
Sample	System	T/W[a]	R_G(Å)	$M_{w,a}$	$\bar{N}_{SANS}$	System	T/W[a]	R_G(Å)	$M_{w,a}$	$\bar{N}_{SANS}$
A4	A	5/1	63	80 000	2	B	1/5	130	672 000	18
A7	A	5/1	125[b]	234 000	3	B	1/5	130	536 000	7
A4	A′	2/1	62	77 000	2	B′	1/5	70	228 000	6
A7	A′	2/1	69	71 000	1	B′	1/11	240	950 000	13

[a] Ratio toluene/water in the ternary solvent mixture;
[b] In this case, the particles have been shown to form clusters (see papers 1 and 3). Consequently, the reported value may be overestimated because of interference effects

THEORETICAL

Neutron or light scattering experiments of polymer solutions are mainly concerned with the determination of positions of monomers in the systems. For the simplest case of an homopolymer in a macromolecular environment, the coherent scattered intensity $I(q)$ is given by the relation:

$$I(q) = A \cdot M_w C \cdot \nu^2 \cdot P(q) \tag{1}$$

where A is an apparatus constant, and M_w and C are the weight-average molecular weight and the concentration of the polymer, respectively. The coherent scattered intensity $I(q)$ depends on two terms: the contrast factor ν^2, related to the nature of the interaction between the radiation and the monomer in the medium and the normalized structure factor $P(q)$, which is a function of the position of monomers and is given by the relationship:

$$P(q) = \frac{1}{N^2} \sum_{ij} < e^{iq \cdot (r_i - r_j)} > \sim \frac{1}{N^2} \int e^{iq \cdot r} P(r) dr \tag{2}$$

where the quantity N represents the number of monomeric units per chain. The vector $\mathbf{r}_i$ is the position of the i^{th} monomer and the brackets stand for angular and thermal averages. Clearly, $P(q)$ is the Fourier transform of the probability $P(\mathbf{r})$ of having two monomers at a position $\mathbf{r}$.

Study of copolymers composed of unlike chemical sequences is more complicated and involves two types of problem. The first, of a technical nature, arises from the contrast factor between copolymer chains and the surrounding medium. In the case considered here, the problem is still more intricate since the solvent itself is a mixture. The second, more specific to the copolymer structure, concerns the calculation of the form factor. Although these two problems are closely connected, we will consider them separately and show how they can be solved.

Contrast problem

In light scattering experiments, the contrast factor depends on the difference of refractive indexes between monomers and solvents. Moreover, in solvent mixtures, we have to take into account the preferential absorption effect which modifies the solvent composition in the immediate neighbourhood of the polymer.[11]

In neutron scattering experiments, it is relatively easy to overcome the latter difficulty. The contrast factor ν is an apparent coherent scattering length of the monomer in the medium and is given by:

$$\nu = \bar{V}_m (b'_m - b'_s) \tag{3}$$

where $\bar{V}_m$ is the specific volume of monomers, b'_m and b'_s are the coherent scattering lengths per unit volume of monomers and solvent, which depend only on the nuclear structure. Then, mixtures of H and D species of the same solvent provide different contrast factors without significantly changing the physicochemical properties.[12]

When dealing with a solvent mixture, we can keep the scattering length b'_s of the solvent mixture constant, whatever its composition, by suitably adjusting the respective amounts of H and D species of each component. In the case considered here, the scattering length of the water/toluene/2-propanol mixture has been adjusted to that of deuteriated toluene. The latter has a value intermediate between those of H and D species of 2-propanol and water (see scale reported in *Figure 1*). This situation has been obtained for the following compositions (% w/w). Water: H 9.5/D 90.5 - 2-propanol: H 8.3/D 91.7 - toluene: H0/D100.

Consequently, one can consider the solvent medium as a unique solvent and thereby reduce the problem to the case of a two sequence copolymer (AB) incorporated in a surrounding S.

For such systems, equation (1), giving the scattering intensity, can be written as a function of the apparent molecular weight and of the apparent form factor, according to:

$$I(q) = A \cdot M_{app} \cdot C \cdot \bar{\nu}^2 \cdot P_{app}(q) \tag{4}$$

where $\bar{\nu}$ is the average contrast factor of the copolymer defined as:

$$\bar{\nu} = x\nu_A + (1-x)\nu_B \text{ and } \nu_A = \bar{V}_A(b'_A - b'_s), \quad \nu_B = \bar{V}_B(b'_B - b'_s) \tag{5}$$

with evident significantion of the subscripts. The parameter x is the weight fraction of the sequence A in the copolymer.

Calculations of the apparent form factor $P(q)$ have already been developed for such polymers, namely:[13]

$$P_{app}(q) = \frac{1}{\bar{\nu}^2} [x^2\nu_A^2 P_A(q) + (1-x)^2 \nu_B^2 P_B(q) +$$

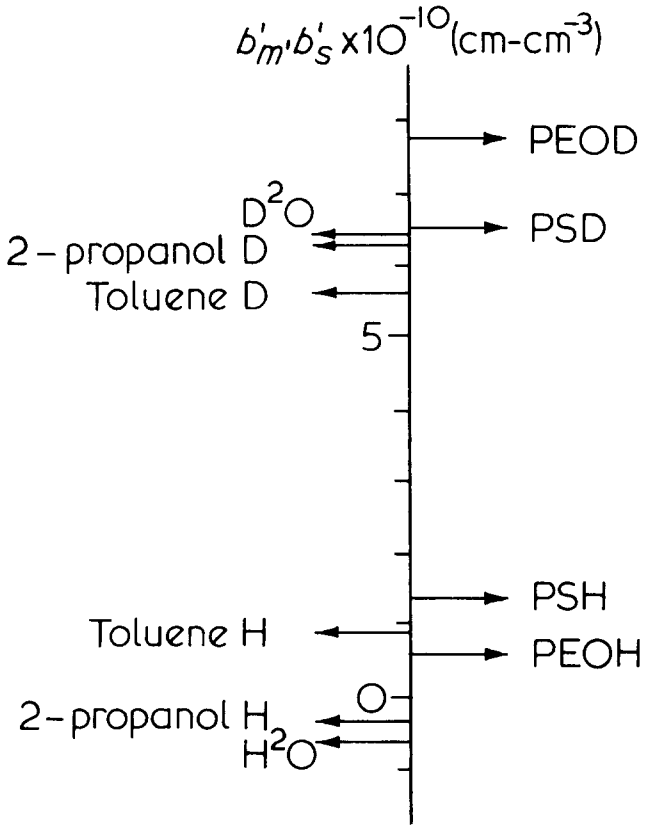

Figure 1 Coherent scattering lengths per unit volume of polymers and solvents

$$+ 2x(1-x)\nu_A\nu_B P_{AB}(q) \tag{6}$$

where $P_A(q)$ and $P_B(q)$ are the form factors of sequences A and B, respectively. $P_{AB}(q)$ is a cross term taking into account interference between the two sequences.

The values of ν obtained for the systems investigated here are the following:

$$\nu_{PS} = -3.98 \times 10^{10}\,\text{cm g}^{-1}$$
$$\nu_{PEO} = -4.15 \times 10^{10}\,\text{cm g}^{-1}$$

and for the copolymers

$$\nu_{A4} = -4.10 \times 10^{10}\,\text{cm g}^{-1}$$
$$\nu_{A7} = -4.07 \times 10^{10}\,\text{cm g}^{-1}$$

For this calculation, we have used the scattering lengths given by neutron tables[14] and the values of the specific volumes of PS[15] and PEO[16] measured in the bulk and in a good solvent, respectively:

$$\bar{V}_{PS} = 0.94\,\text{cm}^3\,\text{g}^{-1} \qquad \bar{V}_{PEO} = 0.83\,\text{cm}^3\,\text{g}^{-1}$$
$$b'_{PSH} = 1.41 \times 10^{10}\,\text{cm cm}^{-3} \qquad b'_{PEO} = 0.685 \times 10^{10}\,\text{cm cm}^{-3}$$

We observe that $\nu_{PEO}/\nu \simeq \nu_{PS}/\nu \simeq 1$ for both A4 and A7 samples, so that $P_{app}(q)$ whatever the composition of PS-PEO copolymers i.e.:

$$P(q) \simeq x^2 P_A(q) + (1-x)^2 P_B(q) + 2x(1-x)P_{AB}(q) \tag{7}$$

This result means that, as far as the contrast is concerned, the copolymer can be considered as an homopolymer. This emphasizes the considerable advantage of neutron scattering over light scattering for such a complex system.

Form factor

The form factor can be calculated for different types of scatters and two domains of q are particularly interesting.

(1) In the Guinier range ($q \cdot R_G \leqslant 1$), we observe that the long-range correlation between monomers and $I(q)$ can be written as:[17]

$$I(q) = AM_wC\nu^2\left(1 - \frac{q^2R_G^2}{3}\right) \tag{8}$$

In the general case of a two component polymer, the radius of gyration and the molecular weight are apparent quantities. However, as shown above for the systems investigated here, we do measure the real dimensions.

(2) In the intermediate range $R_G^{-1} \leqslant q \leqslant l^{-1}$, one observes the short range intrachain correlations. The $P(q)$ behaviour gives the details of the form of the chain and can be expressed as $P(q) = \text{constant}/q^n$ where n is a characteristic exponent of the chain conformation.[18]

For rod-like structure, $n = 1$; Gaussian chains, $n = 2$; three-dimensional excluded volume, $n = 5/3$; isolated collapse chains below the theta point, $n = 3$; hard spheres, $n = 4$. (9)

In some cases, $P(q)$ may exhibit two well-defined behaviours in the intermediate range. This has been particularly pointed out for semi-dilute homopolymer solutions.[9] The scattering vector q^* at which the cross-over occurs is an important characteristic of the chain conformation.

Calculations of the form factor for unlike sequences of copolymers are rather complicated since each sequence interacts differently with the surrounding solvent. Two limiting situations have already been discussed.

(a) *Comb-shaped homopolymers in a θ solvent.*[19,20] The form factors of random combs have been calculated by Casassa and Berry[20] who give the following expression:

$$P(q) = \frac{2}{u^2}\left\{u - (1-e^{-u\lambda}) + (1-e^{-u(1-\lambda)/f}) \times \left[f - \frac{2(1-e^{-u\lambda})}{u\lambda/f}\right] + (1-e^{-u(1-\lambda)/f})^2\left[\frac{u\lambda - (1-e^{-u\lambda})}{u^2\lambda^2/f(f-1)}\right]\right\} \tag{10}$$

In this equation: $u = q^2R_G^2$ where R_G is the radius of gyration of a linear macromolecule of the same molecular weight, λ is the fraction of the main chain (N_0 segments) in the molecule (N segments) and f the number of branches.

We have computed some theoretical curves deduced from equation (10) for different molecular structures. They are reported in the classical Kratky[21] representation $q^2P(q) = f(q)$ in *Figure 2*. The function $q^2P(q)$ usually exhibits a peak followed by a slow decrease. In the range of high scattering vector, $q^2P(q)$ reaches the plateau

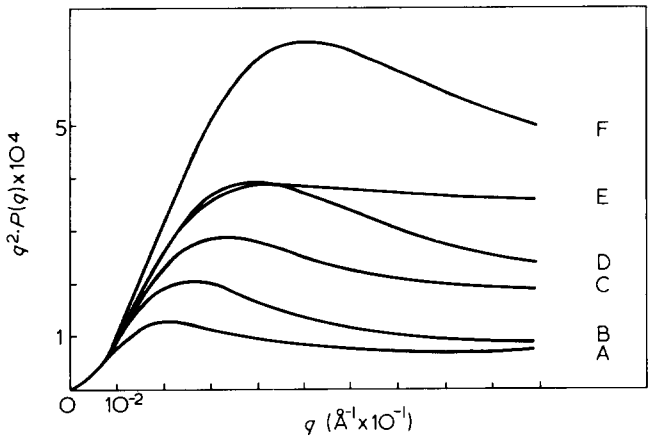

Figure 2 Variation of $q^2P(q)$ as a function of q for PS random comb molecules with various values of λ and f, as calculated from Casassa's and Berry's equation[20] (no. 10 in the text). The values of the radii of gyration R_G are deduced from the relationship R_G(Å) = 0.275 x $M^{0.5}$ given for a linear macromolecule in a θ solvent.[6]
A, N_0 = 175; λ = 0.06; f = 6.5;
B, N_0 = 356; λ = 0.13; f = 13;
C, N_0 = 175; λ = 0.13; f = 6.5;
D, N_0 = 356; λ = 0.27; f = 20;
E, N_0 = 175; λ = 0.25; f = 3;
F, N_0 = 175; λ = 0.29; f = 9

typical of the Gaussian régime for a linear homopolymer. As a general rule, the departure from the q^2 dependence is the more pronounced, the smaller the length of the arms and (or) the interspacing chains. For instance, plotting log$P(q)$ *versus* log$q$ for two structures similar to those of samples A4 and A7 one finds in the high range of $q(> 5 \times 10^{-2}$ Å$^{-1})$ exponents close to 2 and 2.3 respectively.

However, this model seems quite unrealistic for copolymers, since the form factor has been calculated by assuming a Gaussian distribution for all the pair correlations of segments in the molecule. It is clear that in this case there are some strong excluded volume effects between segments of unlike chemical nature, even if both sequences are surrounded by a theta solvent.

(b) *Star-shaped copolymer micelles.*[22] Inagaki *et al.* considered micelles consisting of f molecules of A-B diblock copolymer, where the B subchains form a hard core of radius R_1, surrounded by the soluble A subchains. Their calculations on the apparent form factors $P_A(q)$, $P_B(q)$ and $P_{AB}(q)$ lead to:

$$P_A(q) = \frac{2}{fu_A^2}\left[\exp(-u_A)+u_A-1 + \frac{f-1}{2}\exp(-u_B^2/3)\left\{\exp(-u_A)-1\right\}^2\right] \quad (11a)$$

$u_A = q^2(N_A b_A^2/6)$ where N_A is the number of segments of monomers A in the copolymer and b_A the length of the statistical element.

$$u_B = q^2R_1^2$$

$$P_B(q) = [(3/u_B^3)(\sin u_B - u_B \cos u_B)]^2 \quad (11b)$$

and

$$P_{AB}(q) = (3/u_A)[1-\exp(-u_A)]\exp(-u_B^2/6) \times [(6)^{1/2}/u_B]^3 I_1[u_B/(6)^{1/2}] \quad (11c)$$

$$I_1(y) = \int_0^y t^2\exp(-t^2)dt \text{ with } y = u_B/(6)^{1/2}$$

Two limiting cases can be envisaged: (i) $R_1 = 0$; this case reduces to a regular star model with f branches[23] (excluded volume); (ii) the length of the branches goes to zero; the $P(q)$ function is equivalent to that of a hard sphere.

Clearly, the systems investigated here correspond to situations intermediate to those two limiting cases. However, the Inagaki model is still unrealistic because it neglects (as in the preceding model) the effects of volume exclusion between segments; in particular the A segments are allowed to enter the domain occupied by the B segments.

Equation (11) which in the general case is too complicated to allow a qualitative comparison with experiments, becomes simpler in the high scattering vector limit.

For $q^2R_1^2 \sim q^2(N_A b_A^2/6) \gg 1$ we have:

$$P_{AB}(q) \text{ and } P_B(q) \ll P_A(q) \sim \frac{2}{fu_A} \sim q^{-2} \quad (12)$$

The above relationship shows that, for scattering vectors much larger than the dimensions of both the side branches and the central core, the asymptotic behaviour is controlled only by the side branches surrounding the core. In the Inagaki model, it obeys the Gaussian régime of a linear homopolymer and in a model with excluded volume effects, it should presumably follow the typical $q^{-5/3}$ dependence.

On account of the complexity of the systems, we will restrict ourselves to the study of the apparent exponents in the different momentum ranges, in order to obtain information on the compactness and local conformation of molecules.

RESULTS

The determination of the radius of gyration and the molecular weight of the dispersed particles requires an extrapolation to zero concentration. One of the major problems encountered in the investigation of micellar systems concerns the choice of the dilution solvent. This solvent must have the same composition as that of the continuous phase in the medium. Such information has been obtained from the dialysis experiments as reported in the preceding paper. We will see later that the structure of the micelles is unaffected by this dilution process.

Radii of gyration and molecular weights of copolymers enclosed in the micelles are determined from the classical Zimm representation[24] of the data obtained in the Guinier range ($q \cdot R_G \leqslant 1$ (*Table 1*). An example, relative to sample A4 is given in *Figure 3*. The radius of gyration is obtained from the slope of the straight line $c/I = f(q^2)$ at given concentrations. We observe in *Figure 3* that this slope is independent of the polymer concentration, which means that the radius of gyration does not change under dilution. We should also note the slightly negative value of the second virial coefficient A_2 given by the

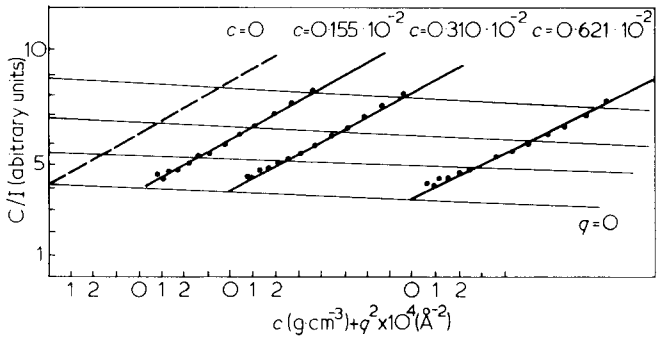

Figure 3 Zimm representation for the system water/toluene sample A4/2 propanol at the overall composition B' (*Figure 4*, paper 1)

slope of $c/I = f(c)$ at given q. This result is evidence for the existence of attractive forces between particles. The molecular weight of the copolymer material within the micelle $M_{w,a}$ is obtained from the intercept at $c = 0$ and $q = 0$. The apparatus constant A has been calculated from measurements on a well-defined polystyrene in deuterated benzene.

Table 1 summarizes the results obtained for the different systems investigated. From the values of $M_{w,a}$ and of the individual molecules M_w, we can calculate the aggregation numbers $\bar{N}$. As a general rule, both dimensions and aggregation numbers increase when the medium grows richer in water.

Contrary to measurements in the Guinier range, the investigation of the asymptotic behaviour does not require an extrapolation to zero concentration. However, a study of $I(q) = f(c)$ provides a good check on the structural stability of micelles in dilution. *Figure 4* shows the scattering vector dependence of the scattered intensity in the intermediate range (sample A4, system B) for two given concentrations varying in a ratio of 32 to one. Although the experimental accuracy is less for the more dilute system because of the lower intensity, we observe the same behaviour for both systems in all the investigated range of q; this shows that there is no significant dilution-induced structural change in the micelle.

The influence of the compositions of both copolymers and ternary solvent mixtures is illustrated in *Figures 5* and *6* where the scattering intensity data have been reported in the classical representation $q^2I(q) = f(q^2)$. In some cases, several régimes are observed, depending on the domain of scattering vector investigated. The crossover between two régimes appears distinctly in a $\log(I) = f(\log q)$ representation, as illustrated in *Figure 7* relative to sample A7 (system A). The characteristic exponents of q can be determined from the slopes of the straight lines.

The values of crossover scattering vector q^* and exponents are reported in *Table 2* for the different systems. A first inspection shows that the asymptotic behaviour of these systems is rather complex and requires a detailed discussion.

DISCUSSION

Before trying to deduce information on the internal structure of the micelles from the results, it would seem useful to describe some general features of these systems.

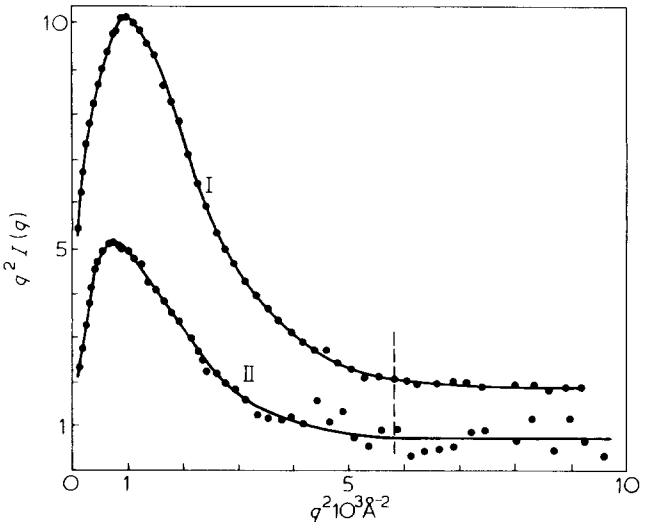

Figure 4 $q^2I(q)$ in arbitrary units is plotted *versus* q^2 for 2 systems relative to copolymer A4 at two concentrations (overall composition B; high water content)
I $c = 3.98 \times 10^{-2}$ g cm^{-3}
II $c = 0.12 \times 10^{-2}$ g cm^{-3}

Crossover of the correlation function P(q)

One of the most interesting observations is the existence in several cases (see *Table 2*) of a well-defined crossover of the form factor $P(q)$ between two different scattering behaviours.

Inspection of *Table 2* shows that this crossover occurs for roughly the same value of q^*, whatever the system investigated. This observation is surprising since the dispersed particles differ considerably in aggregation number and degree of swelling. An illustrative example is given by the copolymer A7 which exhibits a crossover from a Gaussian (system A) or a collapsed régime (system B) to an excluded volume régime at the same value of q^*($q^* = 5.45 \times 10^{-2}$ Å^{-1}). This suggests that the crossover is somehow related to the local structure of the copolymer. We will therefore attempt to establish a correlation between q^* and the structural characteristics of the scattering objects.

The morphology of graft copolymers can be described by two characteristic lengths; the length of the PEO graft $M_{w,b}$ and the distance $M_{w,f}$ between two subsequent branches along the PS backbone. From the structural characteristics of samples A4 and A7 (see *Table 1*, paper 1) we obtain the following values of the molecular weights associated with these two parameters (*Table 3*). The lengths corresponding to these chain elements are quite difficult to evaluate since the state of solvation in the different systems considered here is unknown. The dimensions of PEO molecules in aqueous solutions[25] and those of PS in a θ solvent[26] have previously been determined by neutron scattering. In *Table 3*, the values of the radii of gyration $(\bar{R}^2)^{1/2}$ and the mean end-to-end distances $(\bar{r}^2)^{1/2}$ obtained for molecules of same molecular weights as PEO branches and PS interspaced chains are reported.

The crossover scattering vector, q^*, defines a characteristic distance ξ which can be calculated as in the case of semi-dilute solutions:[27]

$$\xi = q^{*-1} \qquad (13)$$

Table 2 Values of the exponent n in the relationship $P(q) = \frac{\text{constant}}{q^n}$

	Sample A4			Sample A7		
	n ($q < q^*$)	q^*(Å^{-1}) (crossover)	n ($q > q^*$)	n ($q < q^*$)	q^*(Å^{-1}) (crossover)	n ($q > q^*$)
Toluene-rich area:						
Transition line (A)	1.96	–	1.96	1.92	5.45×10^{-2}	1.68
Upper domain (A')	3.04	–	3.04	2.3	6×10^{-2}	1.60
Water-rich area:						
Transition line (B)	4.4	7.6×10^{-2}	2.3	2.9	5.45×10^{-2}	1.62
Upper domain (B')	4.3	–	4.3	3.5	$4\,4 \times 10^{-2}$	2.7

In fact, there is some uncertainty in the definition of q^*, since the change of behaviour of $P(q)$ occurs in a cross-over domain. SANS experiments on semi-dilute polymer solutions in good solvents have shown that, depending on the ξ determination procedure,[27] one must use either equation (13) or:

$$\xi = 1.55 \times q^{*-1} \qquad (14)$$

The values of ξ obtained from equations (13) and (14) are reported in *Table 3*.

It is difficult to reach a clear-cut conclusion from comparison between ξ and the structural parameters of copolymer molecules; it is not clear whether ξ should be compared to the radius of gyration or the mean end-to-end distance. However, inspection of *Table 3* shows unambiguously that ξ is certainly smaller than the dimensions of PEO side branches. Furthermore, ξ is of the same order of magnitude as the interspacing between branches. The latter point is of importance, since one can reasonably assume that for spatial scales smaller than the interspacing distance, the 'comb effects' will be attenuated and the behaviour of $P(q)$ will approach that of a linear macromolecule.

Overall behaviour ($q < q^*$)

The investigation of the structure factor in the domain $q < q^*$ provides information on the overall conformation of the dispersed particles. From inspection of *Table 2*, one observes that the exponent n of the curves $q^2I(q)$ ranges from 1.92 to 4.3. This result shows that there are no apparent long-range exluded volume effects but that the chains adopt a conformation varying from statistically Gaussian to hard sphere depending on the amphiphilic nature of the copolymer and the composition of the solvent mixture as discussed below.

Influence of the copolymer structure. Sample A4 which contains a lower proportion of PEO is generally more compact than sample A7. This is particularly clear in water-rich systems for which sample A4 exhibits a hard sphere behaviour ($n \sim 4.3$) whereas sample A7 is chain collapsed ($n \sim 3$). This compact behaviour is in accord with a high aggregation number ($6 < \bar{N} < 18$).

Influence of the solvent mixture composition. The particles exhibit a more compact structure in the water-rich side than in the toluenic-side of the phase diagram. In the latter case, we observe for system A the characteristic Gaussian behaviour of a linear macromolecule. This result suggests that both sequences are surrounded by a theta-like mixture corresponding to a balanced composition of precipitant and solvent. We have seen that such a situation should lead, for comb-shaped homopolymers, to an apparent exponent of $P(q)$ higher than 2.[20] However, the model does not account for the incompatibility between the two sequences which may produce a cancellation of comb effects. Consequently, the contribution to the form factor arising from the branch subchain and the backbone, respectively can be expected to be additive.

Excluded volume effects ($q > q^*$). *Figures 5* and *6* and *Table 2* show that sample A7 exhibits for all but one of the investigated systems, an asymptotic behaviour of $I(q)$, characteristic of the excluded volume régime. This effect, to be discussed later, may be related to the structure of the micelles. The incompatibility between the PS backbone and the PEO arms of the copolymer produces an intramolecular phase separation. In addition, the segregated molecules may undergo intermolecular association forming stable micelles.

We believe that the main excluded volume effect originates in the PEO layer for the following reasons.

(a) As mentioned above, the two copolymer sequences present the same contrast for SANS; thus the neutrons 'see' essentially the PEO component as it forms 74% of sample A7.

(b) The amount of (water + 2-propanol), both good solvents of PEO, greatly exceeds that of toluene in all the systems considered here.

(c) The aggregation numbers are rather high for predominantly aqueous systems. This is not surprising since water is a very strong precipitant for polystyrene. It is then unlikely that the PS core of such aggregates exhibits even a local expansion. The Inagaki model[22] predicts that for such conformations, the major contribution to $P(q)$ arises from side branches provided that $q^2R_1^2 > 1$ and $q^2R_A^2 > 1$ (see above). This is the case considered here ($q > q^*$), as can be ascertained from the comparison between the values of ξ and those of the characteristic dimensions of the copolymer subchains (see *Table 3*).

(d) The crossover scattering vector q^*, beyond which the excluded volume appears, does not depend on the location of the system in the phase diagram. This suggests that the excluded volume originates in the sequence least affected by a change in the ternary

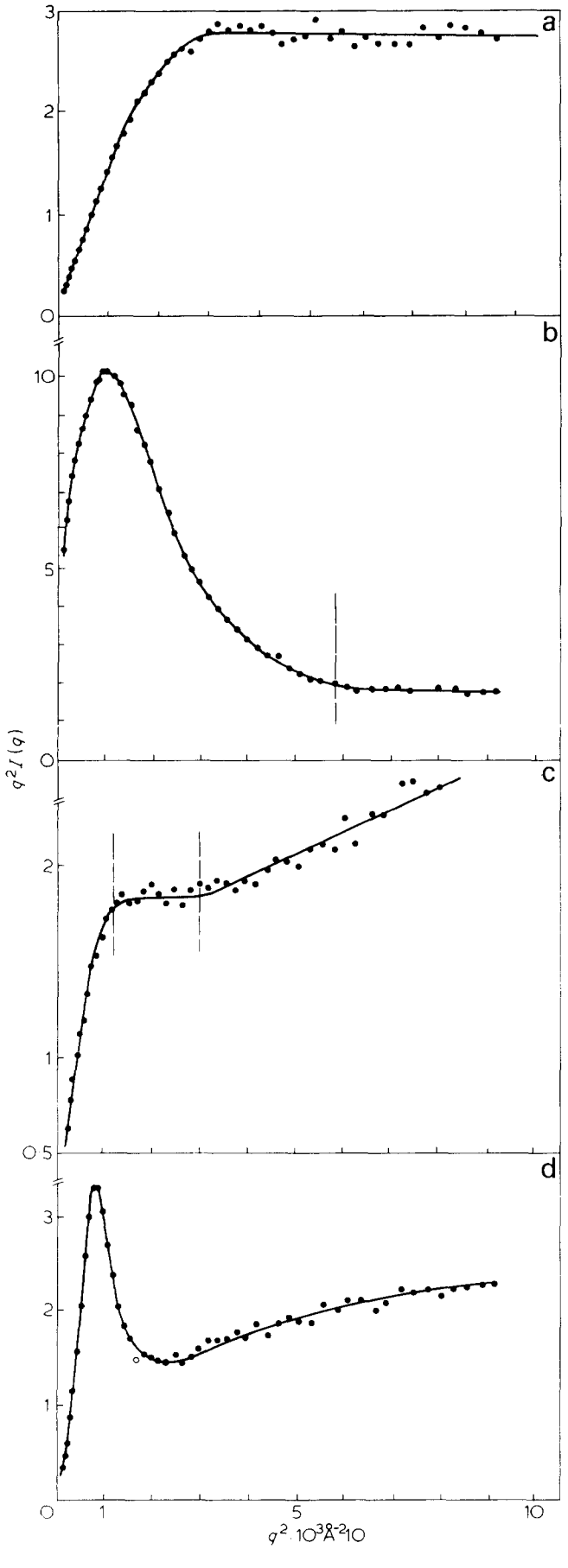

Figures 5(a)-(d) $q^2 I(q)$ in arbitrary units as a function of q^2 for the systems relative to samples A4 and A7 (overall compositions A and B at the transition line). The copolymer concentration is $C = 3.98 \times 10^{-2}$ g cm^{-3}

mixture composition. This sequence is clearly the PEO for the reasons mentioned above.

Based on these considerations, we can attempt to give a physical insight into the characteristic length ξ. If the PEO layer has a degree of swelling such that all the PEO side branches are mutually excluded, ξ should be of the order of magnitude of the radius of gyration of the PEO graft. However, the junction points of side branches are rather close to each other along the PS backbone. As a consequence, the mean PEO concentration $\langle C \rangle$ in the external shell may be high enough to produce contacts between branches (as shown schematically in *Figure 8*). In this case (similar to that of semi-dilute polymer solutions for a good solvent), the characteristic length is smaller than the radius of gyration of the branch and depends only on the mean PEO concentration, according to:[28]

$$\xi = R_G \left(\frac{\langle C \rangle}{C^*} \right) - 0.75$$

where C^* is the monomer concentration in a single branch: $C^* \simeq M_{w,b}/R_b^3$.

Of course, in the systems considered here, there will be a contribution due to PS but it will be overcome by that of PEO, because of the copolymer composition. Moreover, since the size of PEO side branches is quite large, they could exert a repulsive interaction strong enough to produce a local expansion of the PS backbone. The excluded volume effect should then be enhanced in the high momentum range, since there will be excluded volume contributions from both backbone and branches.

Finally, we must discuss the results obtained for sample A4 which does not exhibit any excluded volume effect. Two reasons may be invoked to explain this behaviour.

First, the weight ratio PS/PEO is much larger for sample A4 than for sample A7. Thus the PS core might require a more concentrated PEO outer layer in order to protect itself from the external precipitant as suggested by the higher aggregation number in system B. Therefore, the PEO shell tends to adopt a more compact conformation, either Gaussian or collapsed. Furthermore, the contribution of PS to $P(q)$ is more important than for A7.

Alternatively, the length of the A4 side branches is much smaller than that of sample A7. It has been shown theoretically[29] and experimentally[30] that the theta domain of a polymer chain is as much extended as the molecular weight of the chain is decreased and as the concentration is increased. Thus, the side branches of both samples might exhibit a different conformational behaviour even in the same surroundings.

Structure of micelles

A schematic description of the copolymer micelles can now be made. The medium outside of the micelles is a good solvent for PEO, even for large T/W ratios, thus the PS backbones would accumulate in the core and the more soluble PEO side branches would protect the micelles from further aggregation. *Figure 9* shows examples of plausible micellar models which account for the relative variation of the radius of gyration, the aggregation number and the asymptotic behaviour of the form factor.

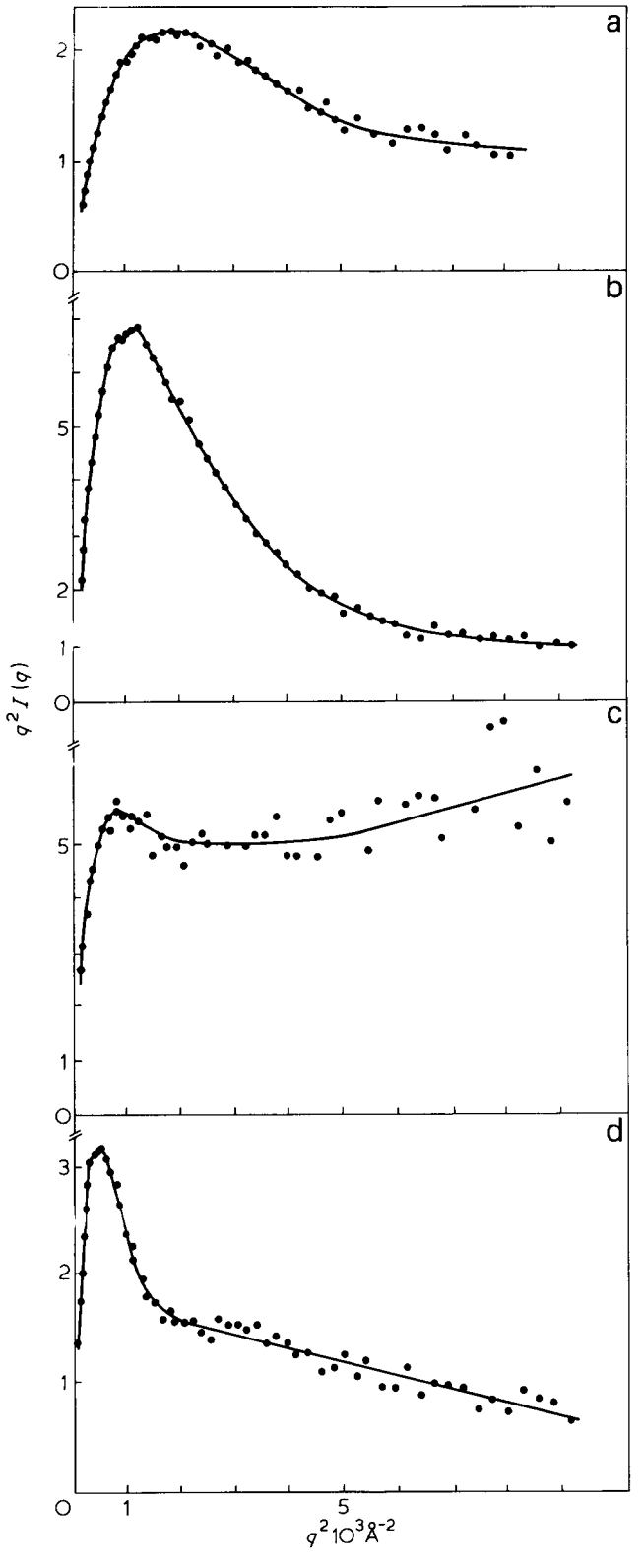

Figures 6(a)–(d) $q^2I(q)$ in arbitrary units *versus* q^2 for the systems relative to samples A4 and A7 (overall compositions A′ and B′, high 2-propanol content).
(a), (b), (d): the copolymer concentration is $C = 0.618 \times 10^{-2}$ g cm^{-3}
(c): $C = 0.301 \times 10^{-2}$ g cm^3

System A. System A which contains a rather high percentage in toluene. The micellar structure is quite similar for either sample A4 or A7. The aggregation number is low, (~2) the core is swollen by a predominantly toluene-rich mixture in which the PS chains adopt a Gaussian conformation. The only distinct difference of behaviour concerns the conformation of PEO chains which exhibit an excluded volume effect in the short distance range for sample A7 ($n \sim 1.68$) and a Gaussian régime for sample A4 ($n \sim 1.96$). This may be attributed to the smaller length of the side branches as discussed in the preceding paragraph. As for the PS core, its swelling should be approximately the same for both samples, since similar aggregation numbers and overall behaviour is observed for $P(q)$.

System B. We now turn to a description of the structural change which occurs when toluene is replaced by water, i.e. when going from system A to system B. Because of the worsening of the quality of solvent for PS, there is an increase of the aggregation number which is more pronounced for sample A4 (~18) than for sample A7 (~7). This aggregation process is accompanied by a drastic change of the conformation of PS chains, as shown by the overall behaviour of $P(q)$. The A4 PS chains are precipitated and form a hard core in the micelle ($n \sim 4.3$). For systems obtained from sample A7, the exponent ($n \sim 3$) of $P(q) = f(q)$ is rather indicative of a collapsing of the chain.

On the other hand, the external PEO shell is little affected by the change in the continuous phase composition since the same asymptotic behaviour of $P(q)$ is observed in both systems A and B. Moreover, the equality observed for sample A7 between the two crossover values ($q^* = 5.45 \times 10^{-2}$ Å^{-1}) indicates that the PEO concentration in the shell is the same on both sides of the phase diagram in spite of a larger number of side branches in system B. This result can only be obtained by a swelling of the chain.

Systems A′ and B′. Before closing this section, we comment on the results obtained for systems containing an excess of 2-propanol. By addition of 2-propanol which is a precipitant for PS, a considerable increase of the compactness of the micelles is observed for the more hydrophobic copolymer. i.e. sample A4 (49% PS). This effect is particularly clear for predominantly toluene-rich phases for which the exponent n goes from the Gaussian value (~1.96), system A) to the collapsed régime value (~3, system A′).

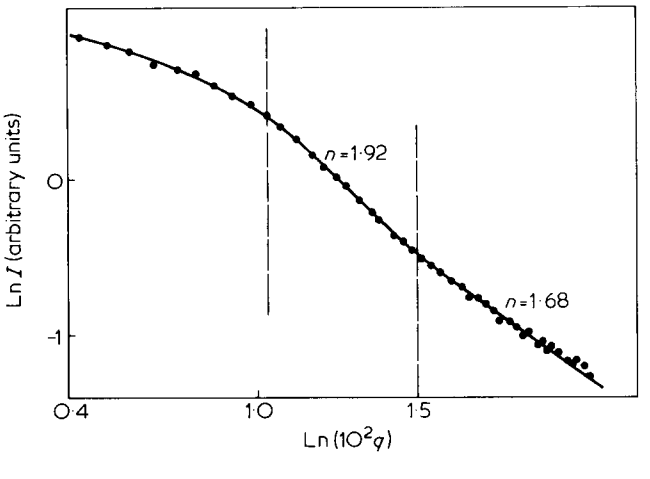

Figure 7 Log–log plot of the scattered intensity *versus* q for a system relative to sample A7 at the composition A (high toluene content). The copolymer concentration is $C = 3.98 \times 10^{-2}$ g cm^{-3}

Table 3 Structural parameters of graft copolymers as compared to the correlation length ξ

Sample	$M_{w,b}$ (one branch)	$(\bar{R}_b^2)^{1/2}$ Å	$(\bar{r}_b^2)^{1/2}$ Å	$M_{w,f}$ (between 2 branches)	$(\bar{R}_{0,f}^2)^{1/2}$ Å	$(\bar{r}_{0,f}^2)^{1/2}$ Å	$\xi = q^{*-1}$ (Å)	$\xi = 1.55q^{*-1}$ (Å)
A4	2100	17	41.7	2020	11	27	13.2	20
A7	7800	44	107.8	2800	14	34	18.4	28

As for sample A7 (26% PS), its conformation is not very affected by the transition from system A to A'.

The case of the system B' relative to sample A7 (see *Figure 9*) has to be considered separately as a limiting case, since the solvent mixture is composed of 31.9% water 65.2% 2-propanol but only 2.9% toluene. This medium is so unfavourable for PS that it imposes a large aggregation number in order to realize an efficient protection of the core and the structure then becomes quite compact.

CONCLUSION

The results presented in this paper provide a semi-quantitative description of the dispersed phase of quaternary systems stabilized by amphiphilic copolymers. The dimensions and the aggregation numbers of the micellar droplets have been estimated as a function of the copolymer composition and the location of the system in the phase diagram. In addition, the short range structural characteristics have been obtained from the asymptotic behaviour of the scattering from factor $P(q)$. The latter has been found not to vary with the copolymer concentration, thus confirming the validity of our dilution procedure.

The experimental data can be accounted for in the whole phase diagram by a model of segregated micelles with a PS core surrounded by the solvated PEO grafts. The formation of reverse micelles (with a PEO core) was shown to be very unlikely even in toluene-rich mixtures.

The micellar structure depends primarily on two factors: the weight fraction R of PS in the copolymer and the toluene fraction X in the toluene-water mixture. On average, large R and low X values lead to compact and aggregated micelles, small R and large X values to a coil conformation of the copolymer in the micelle and to small aggregation numbers. A further step for a more accurate description of the structure of these dispersed particles would be accomplished by selectively labelling either the side branches or the backbone of copolymer molecules.

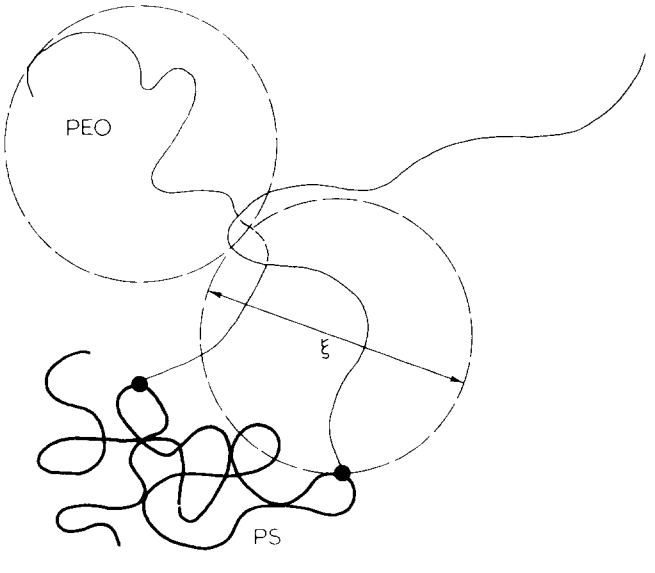

Figure 8 Partial sketch of a micelle. Excluded volume effects occur for distances lower than ξ

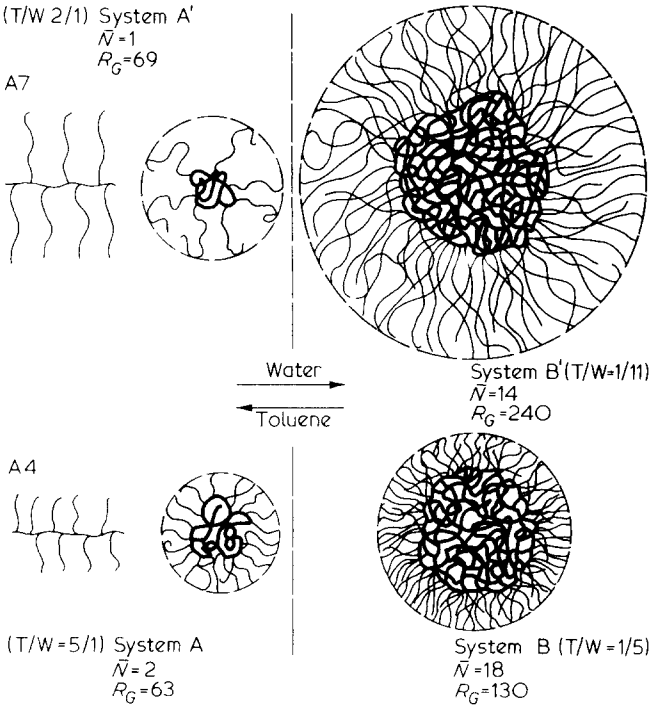

Figure 9 Schematic representation of the copolymer micelles for sample A7 (systems A' and B') and sample A4 (systems A and B)

ACKNOWLEDGEMENTS

The authors wish to thank Professor H. Benoit and Professor R. Ullman for stimulating discussions and Dr R. Duplessix for helpful assistance during the experiments.

REFERENCES

1 Candau, F., Boutillier, J., Tripier, F. and Wittmann, J.C. *Polymer* 1979, **20**
2 Hoar, T.P. and Schulman, J.H. *Nature* 1943, **152**, 103
3 Shinoda, K. and Friberg, S. *J Colloid Interface Sci* 1975, **4**, 281

4 Dvolaitzky, M., Guyot, M., Lagües, M., Le Pesant, J.P., Ober, R., Sauterey, C. and Taupin, C. *J Chem Phys* 1978, **69**, 3279
5 Kirste, R.G., Kruse, W.A. and Schelten, J. *Makromol Chem* 1973, **162**, 299
6 Cotton, J.P., Decker, D., Benoit, H., Farnoux, B., Higgins, J., Jannink, G., Ober, R., Picot, C. and des Cloizeaux, J. *Macromolecules* 1974, **7**, 863
7 Duval, M., Duplessix, R., Picot, C., Decker, D., Rempp, P., Benoit, H., Cotton, J.P., Jannink, G., Farnoux, B. and Ober, R. *J Polym Sci (Polym Lett Edn)* 1976, **14**, 585
8 Ionescu, L. *Thesis* Strasbourg (1976)
9 Daoud, M., Cotton, J.P., Farnoux, B., Jannink, G., Sarma, G., Benoit, H., Duplessix, R., Picot, C. and de Gennes, P.G. *Macromolecules* 1975, **8**, 804
10 Ibel, K. *J Appl Cryst* 1976, **9**, 296
11 Strazielle, C. and Benoit, H. *J Chim Phys* 1961, **59**, 675
12 Strazielle, C. and Benoit, H. *Macromolecules* 1975, **8**, 203
13 Benoit, H. and Wippler, C. *J Chim Phys* 1960, **57**, 524
14 (a) Bacon, G.E. 'Neutron Diffraction' Oxford, 1962; (b) Turchin, V.P. 'Slow Neutrons' *Israel Prog Sci Trans* 1965 (c) M.I.T. Tables, Feb Apr, 1971
15 Heller, W. *J Polym Sci (A2)* 1966, **4**, 209
16 Hert, M. and Strazielle, C. *Eur Polym J* 1973, **9**, 543
17 Guinier, A. 'Théorie et technique de la Radiocristallographie, Cornell University Press, Ithaca, NY, 1969
18 Guinier, A. and Fournet, G. 'Small Angle Scattering of X-rays', Wiley, New York, 1955
19 Ruscher, C. and Dautzenberg, H. *Faserforsch Textiltech* 1965, **16**, 1
20 Casassa, E.F. and Berry, G.C. *J Polym Sci (A-2)* 1966 **4**, 881
21 Kratky, O. *Kolloid Z* 1962, **182**, 7
22 Tanaka, T., Kotaka, T. and Inagaki, H. *Polymer J* 1972, **3**, 338
23 Benoit, H. *J Polym Sci* 1953, **11**, 50
24 Zimm, B.H. *J Chem Phys* 1948, **16**, 1093
25 Picot, C. Personal communication, 1978
26 Ballard, D.G., Rayner, M.G. and Schelten, J. *Polymer* 1976, **17**, 349
27 Farnoux, B. *Thesis Ann Phys* 1976, **1**, 73
28 De Gennes, P.G. *J Polym Sci (Polym Lett Edn)* 1977, **15**, 623
29 Daoud, M. and Jannink, G. *J Physique* 1976, **37**, 973
30 Cotton, J.P., Nierlich, M., Boué, F., Daoud, M., Farnoux, B. Jannink, G., Duplessix, R. and Picot, C. *J Chem Phys* 1976, **65**, 1101